

Study the Effect of the Diameter of Annular Parachute on Drag Using CFD

Haifa El-Sadi, Eric Kruzyk, KM Ashik and Chris Alcantara
Wentworth Institute of Technology
550 Huntington, Boston, USA elsadih@wit.edu

Abstract - Parachutes are made of highly deformable fabrics. These fabrics can deploy under many different conditions where the payload must decelerate to a velocity that allows it to survive once it reaches the ground. Understanding the dynamic behavior of parachutes is complex. The problem with modeling parachutes in descent is the challenge of coupling equations involving the unsteady airflow acting around the parachute and the structure of the parachute itself. Because the airflow acting around the parachute is dependent on the parachute's geometry which changes at any given moment of flight, fluid-structure interaction modeling is most appropriate approach to analyzing the parachute behavior. The objective of this project is to investigate the effects of air resistance on annular parachutes of varying diameters. The data and accompanying CFD is analyzed to compare experimental drag force and simulation drag force results. The testing of these parachutes takes place in a wind tunnel, where conditions are controlled and can be matched up with CFD simulations. This will allow us to understand the characteristics of the parachute under steady state conditions.

This data was within 10% at the 25% speed. From the error percentages observed for the given diameters the 4.0 inch has the best results between the experimental and CFD values. While every other model's error percentage goes up along with the speed, the 4.0 inch decreases its error percentage. Although the error percentages could be due to improper test equipment's, the 4.0 diameter has the best data from the given models, leading us to conclude that it is the best diameter for the annular parachute designed. The experimental drag force for the 4.75-inch diameter parachute model at 25% speed was 0.26 Newtons, at 50% speed was 1.53 Newtons and at 75% speed was 3.69 Newtons. The CFD results for drag force at 25% was 0.245 Newtons, at 50% speed was 1.005 Newtons and at 75% speed was 2.218 Newtons. This yielded an error of 5.708% at 25% speed.

Keywords: Parachute, CFD, Drag, Wind Tunnel, steady state

1. Introduction

Man has been fascinated by the idea of flight since at least the renaissance period. Back then, people believe that human flight would resemble bird flight, with people flapping wings to gain lift[4]. In as early as the 12th century, the Chinese could be seen using objects resembling parachutes as a form of entertainment. [9] They would perform stunts in ceremonies and can even be credited to the creation of the umbrella which has an amazing resemblance to a parachute device. As the future presented itself, the interest of aerodynamic decelerators offered an opportunity to bring man safely to the skies. In the 15th century in Italy, Leonardo Da Vinci began making his famous drawings of helicopters and other advanced mechanical devices. One of his drawings from 1485 depicted an idea that resembled today's parachutes [4]. It was not until the 18th century that substantiating evidence of the use of parachute like devices were seen. In France, Joseph Montgolfier threw animals off buildings and eventually himself, which validated their use for humans [9]. Similarly, Sebastion Lenormand demonstrated a jump in Paris which eventually led to the mass attraction of parachute jumping. Presently, aerodynamic inflatable decelerators (AIDs) have been used across space missions to decelerate space crafts at different Mach numbers and varying atmospheric conditions [11]. These complicated parachute devices incorporate complex geometries to support heavy payloads and dynamic pressures. Over the years, parachutes have been used to decelerate objects (both falling or moving) at high speeds. These parachutes all carry different designs that affect how the rate of the intended objects slow down. It is our job in this lab to investigate the different geometries of parachutes and how affective they are. Parachutes are made of highly deformable fabrics. These fabrics can deploy under many different conditions where the payload must decelerate to a velocity that allows it to survive once it reaches the ground [1]. Understanding the dynamic behavior of parachutes is complex. The traditional approach to designing

a parachute is semi-empirical. Due to the amount of time and money this method takes, it is easier to perform computer simulations to reduce cost and get a better design process [2]. To design an efficient parachute system, the interaction of the parachute and the surrounding flow field is important. By using this interaction, it is easier to predict the fluid-structure interactions of a parachute system [1]. Fluid-structure interaction is involved in initial deployment, inflation, terminal descent, and soft landing [1]. By using coupled, nonlinear, and time dependent equations we can understand the different stages of a parachute operation. During the first two stages the parachute deploys and inflates which allows the parachute to decelerate. The terminal descent stage corresponds to everything that happens during the inflation and the input from the user onto the parachute system [2]. By using solidworks the team will model different shapes of parachute systems with alternative dimensions. By using fluid-structure interaction (FSI), the team can understand the best interaction between the parachute system and surrounding flow field to increase efficiency of a parachute system. The testing of these parachutes will take place in a wind tunnel, where conditions are controlled and can be matched up with CFD simulations. This will allow us to understand the characteristics of the parachute under steady state conditions. From here, we can better define the flow American Institute of Aeronautics and Astronautics 3 characteristics in the model to optimize our understanding of the parachute performance. Then, we can decide if the geometry can be further improved and find the force generated to determine the payload weight [6]. This can lead to steady state drop tests with the calculated weights to test the performance of the parachute. This process was used by the Natick Soldier Center on parachutes that are currently in full scale production [6]. Advancements in simulation techniques have allowed engineers to make new developments in parachute performance. The inflated shape of a parachute is a key factor in determining the performance of a parachute. Over time, canopy shape has evolved from “flat circular to conical and then to a quarter spherical and extended skirt design”[5]. Studying axisymmetric-shape parachutes is a good idea, since circular shaped parachutes have been studied extensively in the past. Canopy shapes can be divided into two groups: “free shaped, or pressure shaped parachutes and shaped parachutes that are determined by gore geometry” [5]. A gore is a triangular piece of material. The fuller the gore is, the less tension there is in the canopy material. The problem with modeling parachutes in descent is the challenge of coupling equations involving the unsteady airflow acting around the parachute and the structure of the parachute itself. Because the airflow acting around the parachute is dependent on the parachute’s geometry which changes at any given moment of flight, fluid-structure interaction modeling is most appropriate approach to analyzing the parachute behavior. The Newton-Raphson Method can be used to solve coupled nonlinear equations involving fluid mechanics, structural motion and mesh motion [3]. By assuming that the pressure variation is the same for all geometries, we can use the modeled results as a relative comparison between various shapes [5]. Our primary focus for this project will be on two of the most common parachute types, the ring sail parachute and the ram air parachute. A ring sail parachute is a half sphere shape that connects to the payload with dozens of cords around the edge of the chute. This design is highly scalable and versatile due to its simplicity, ability to handling small payloads as well as heavy cargo and even spacecrafts. The downside to a ring sale parachute is that it lacks any control method and cannot place a payload on ground as accurately. Designs can consist of a large canopy that is broken up by slots in several rings. The slots help to control the deceleration or ‘shock’ felt when the parachute is opened and inflated by allowing the designers to optimize the parachute’s porosity [7]. The ram air parachute is the most aerodynamically efficient out of all the commercially available canopy shapes. The canopy of a ram air parachute is formed of an upper level and a lower level divided horizontally into individual cells that allow air to enter the chambers and inflate the canopy [9]. It’s unique rectangular shape allows the parachute to behave like an airfoil, giving it a large lift to drag ratio and excellent maneuverability. These factors make it an ideal design for applications that require accuracy or direct control from skydivers [10]

2. CFD Analysis

A computational fluid dynamic simulation on parachute models of varying diameters. The fluid was set to air at a temperature of 293.2K and fluid density of 1.225 kg/m³. The type of flow used in these simulations were external using an inlet velocity boundary condition that was coming off a separate body offset from the wide face of the parachute. This separate body was used to resemble the intake of the wind tunnel to match the flow conditions the part experienced during the test. When it came to our goals, we chose to find the average total pressure, the average velocity, the drag force (force in y direction), and we had to make an equation goal for the drag coefficient. The drag coefficient, Cd, was calculated using the following formula. Where V is the velocity of the air, Fd is the drag force.

$$(1) \quad C_d = \frac{2F_d}{\rho V^2 A_{cross \ section}}$$

The computational domain was set to only enclose half of the model with symmetry along the x axis. This still enclosed the whole model in the simulation while only computing half of the model, which the software doubled to account for the non-computed half. This was done to make the computation easier of the software. Designing the mesh involves choosing the geometry of the grid and the number of cells. Common types of meshing include 2-D shapes like triangle and quadrilaterals and 3-D shapes such as tetrahedrons, pyramids, hexahedrons, prisms, and wedges. The discretized equations are solved American Institute of Aeronautics and Astronautics 11 iteratively until they converge to a solution. Good meshing ensures that the simulation quickly and accurately converges. Table of Meshing showing the number of cells, shape of cells, and number of iterations Diameter (in) Inlet Velocity (m/s) Total Number of Cells.

2.1. Boundary Conditions and Analysis

Table 1 revealed the boundary conditions were used for each diameter at different speed percentages.

Table 1. Initial boundary conditions for each parachute diameter

Diameter	Type	Speed Percentage	Value
4.75	Inlet Velocity	25	8.09713051
		50	16.3266275
		75	24.22740946
4.375	Inlet Velocity	25	8.112451489
		50	16.21469543
		75	24.1469792
4.00	Inlet Velocity	25	8.59312196
		50	17.75834698
		75	26.20613176
3.75	Inlet Velocity	25	8.625 m/s
		50	17.9756 m/s
		75	27.056 m/s
3.25	Inlet Velocity	25	7.952711499
		50	16.23892789
		75	24.67179975

Figure 1 shows an example of the flow contour at speed 25% (a) and 75% (b), the flow pattern with speed 25% shows the disturbances in the flow and cause the formation of two vortices that decreased axial velocities. However, when the air speed increased to 75%, non-uniform approach flow to the inlet, shear layers of high velocity gradients and cause more disturbances in the flow. This is the main causes of vortex formation as shown in Figure 1-b.

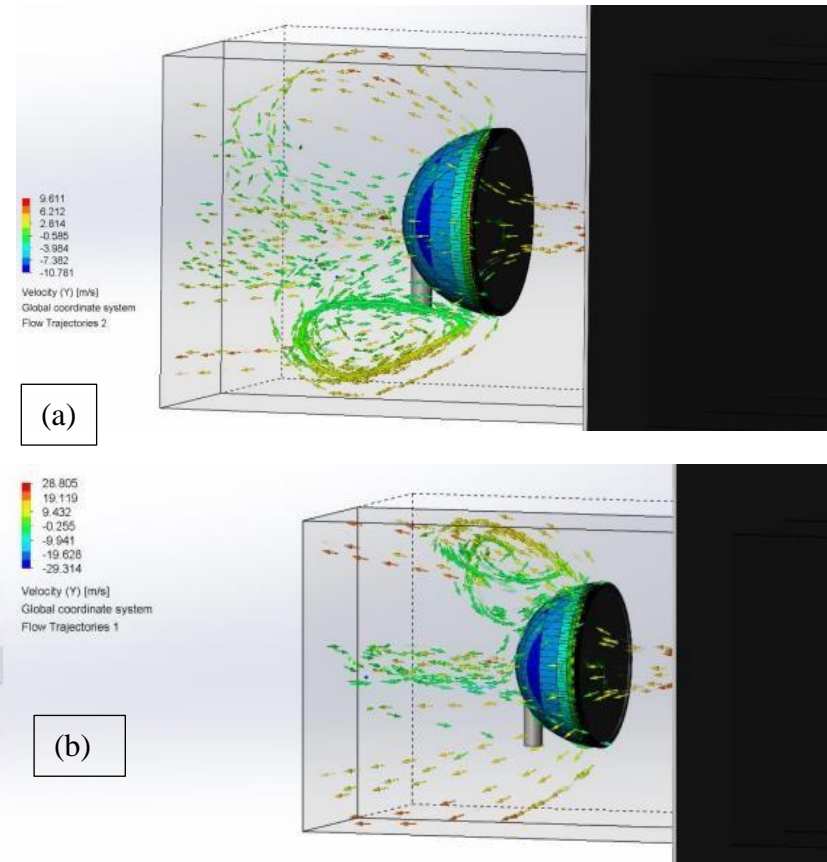


Fig 1. Velocity Contour for 4.375 Inch Diameter (a) 25% speed, (b) 75% Speed

3. BUILDING AND TESTING THE PROTOTYPE

The prototypes were built using 3D printer using PLA filament. These models were tested into a wind tunnel at different wind speeds. Each parachute has a height of 2.375 inches, a thickness of 0.125 inches and a vent hole diameter of 0.75 inches as shown in Figure 2. The diameters of the parachutes vary from 4.75, 4.375, 4.00, 3.75, and 3.25 inches. The parachutes were supported by a 0.125-inch diameter aluminium rod that centred the parachute in the middle of the tunnel for maximum air speed. This rod was fixed to a device that measures the drag force via a 3 point chuck. Using the digital read outs on this device, the drag force values in newtons at the different air speeds were recorded. However, since the stand itself contributes to the drag force, we needed to run a trial with just the 0.125 inch diameter aluminium rod. To have accurate drag force data, the drag force acquired was subtracted during the stand trial from the data acquired during parachute trials. In order to calculate the air speeds, the pitot tube readings are in inches of water and converted to air velocity, this was done using the following equation:

$$v = \sqrt{2g \left(\frac{\rho_{manometer}}{\rho_{working}} \right) \left(\frac{h}{39.37} \right)}$$

(2)

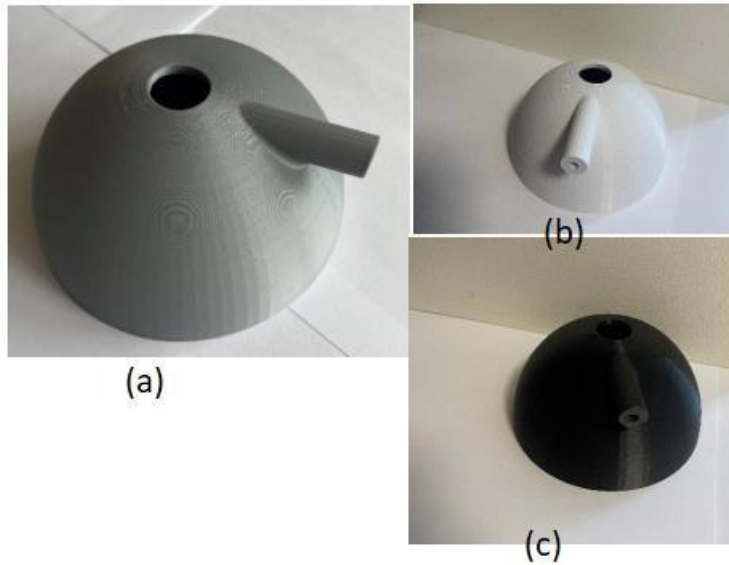


Fig 2. Examples of parachute diameters (a) 4.75 inch, (b) 4.375 inch (c) 4.375 inch

Figure 3 shows that is increasing the parachute diameter leads to increase the drag force at different air speed. On the other hand, drag is increasing with increasing the velocity, however for low air speed the increase in drag with the diameter is insignificant.

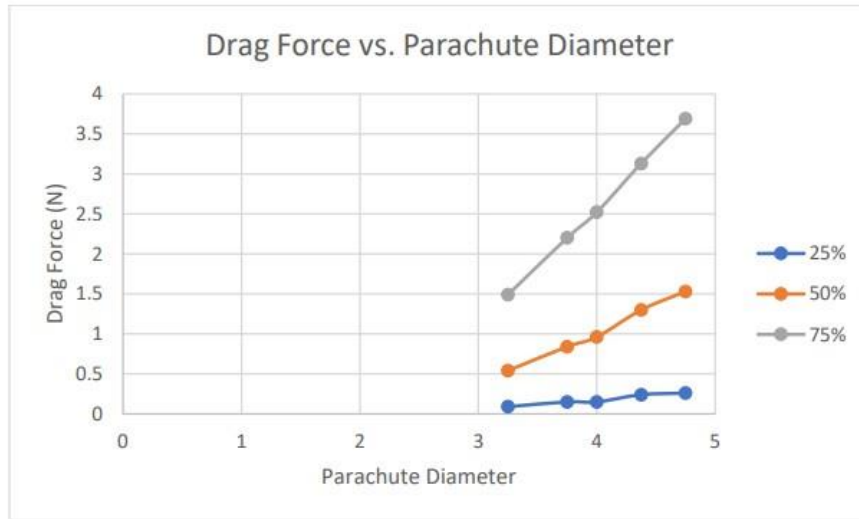


Fig. 3. Drag Force vs. Parachute Diameter.

The parachute models proved to have similar data to the test at the lowest wind speed, but the simulation strayed away from test values as the air speed increased. As the graphs above show, the simulation for all 3 air speeds converged after around 40 iterations. This can be seen as the data after 40 iterations becomes relatively constant and approaches a number without outlying values. The convergence can also be determined from the flow trajectories. The flow trajectories qualitatively make sense with no stray flow vectors in the computational domain. The pressure and velocity also increase with the increase in parachute diameter. For example, the velocity

trajectory graph on the 4.75-inch diameter model at 25% speed has a larger region of low velocity compared to the 3.75 inch diameter model at the same speed percentage. Similarly, the pressure increased as the diameter increased. The pressure on the 4.75-inch diameter model went up to 103576 Pa where the 4.375 inch diameter went to 102136 Pa and the 4.00 inch diameter pressure hit 101836 Pa as shown in table 2.

Table 2. Experimental Results Compared to CFD Results

Diameter	Speed Percentage	Experimental Drag (N)	CFD Drag (N)	Error (%)
4.75	25	0.26	0.245	5.708
	50	1.53	1.005	34.248
	75	3.69	2.218	39.880
4.375	25	0.24	.224	6.667
	50	1.3	.895	31.15
	75	3.13	1.987	36.52
4.00	25	0.15	0.166	10.66
	50	0.96	1.054	9.79
	75	2.52	2.301	8.69
3.75	25	0.15	0.152	1.333
	50	0.84	0.658	21.667
	75	2.2	1.491	32.227

4. CONCLUSION

The results from the CFD simulation were compared to the experimental data by taking the force in the y direction and comparing it to the drag force recorded from the wind tunnel equipment. This data was within 10% at the 25% speed, but the error exponentially increased with the increase in speed percentage. This likely was from the lab equipment itself, since between increasing the speed percentage, the drag force module was not calibrated. Therefore, we believe that the increasing error with increasing speed percentage was due to inaccurate lab equipment. From the error percentages observed for the given diameters the 4.0 inch has the best results between the experimental and CFD values. While every other model's error percentage goes up along with the speed, the 4.0 inch decreases its error percentage. Although the error percentages could be due to improper test equipment's, the 4.0 diameter has the best data from the given models, leading us to conclude that it is the best diameter for the annular parachute designed.

REFERENCES

- [1] Accorsi, Michael, John Leonard, Richard Benney and Keith Stein, "Structural Modeling of Parachute Dynamics." AIAA Journal, vol. 38, no. 1, 2000, pp. 139-146, <https://arc.aiaa.org/doi/abs/10.2514/2.934>, doi:10.2514/2.934.
- [2] Stein, Keith, Richard Benney, Vinay Kalro, Tayfun E. Tezduyar, John Leonard, Michael Accorsi, "Parachute Fluid? Structure Interactions: 3-D Computation." Computer Methods in Applied Mechanics And Engineering, vol.190, no.3, pp. 373-386, <https://www.sciencedirect.com/science/article/pii/S0045782500002085>, doi:10.1016/S0045-7825(00)00208-5.
- [3] Stein, Keith, Tayfun Tezduyar, and Richard Benney. "Computational methods for modeling parachute systems." Computing in Science and Engineering 5.1 (2003): 39-46.
- [4] White, L. (1968). The Invention of the Parachute. Technology and Culture, 9(3), 462–467. <https://doi.org/10.2307/3101655>
- [5] Drozd, Vladimir. "Axisymmetric parachute shape study." 20th AIAA Aerodynamic Decelerator Systems Technology Conference and Seminar. 2009.
- [6] Tutt, B., Richard, C., Roland, S., & Noetscher, G. (2010, June). Development of parachute simulation techniques in LS-DYNA. In 11th international LS-DYNA users conference (pp. 25-36). Livermore Software Technology Corporation.

- [7] Ewing, Edgar G., and Jack R. Vickers. Ringsail parachute design. NORTHROP CORP NEWBURY PARK CA VENTURA DIV, 1972.
- [8] Pazmiño, Angelo A. Fonseca. "A Computational Fluid Dynamics Study on the Aerodynamic Performance of Ram-Air Parachutes." (2018).
- [9] Chernowity, G., ed. : Performance and Design Criteria for Deployable Aerodynamic Decelerators. Patterson AFB. ASD-TR61-579, December 1963.
- [10] Ghoreyshi, Mehdi, Keith Bergeron, Adam Jirásek, Jürgen Seidel, Andrew J. Lofthouse, Russell M. Cummings; "Computational aerodynamic modeling for flight dynamics simulation of ram-air parachutes." Aerospace Science and Technology 54 (2016): 286-301.
- [11] Gillis, C. L. : Aerodynamic Deceleration Systems for Space Missions. ALAA Fifth Annual Meeting, Philadelphia, Penna. October 1968, Paper NO. AIAA 68-1081